Direct Space Representation of the Metallic Bond

Bernard Silvi*

Laboratoire de Chimie Théorique, Université Pierre et Marie Curie, (UMR-CNRS 7616), 4 Place Jussieu 75252-Paris cédex, France

Carlo Gatti

Centro per lo Studio delle Relazioni fra Struttura e Reattività, CNR-CSRSRC, via Golgi 19, 20133-Milano, Italy

Received: August 5, 1999; In Final Form: November 30, 1999

Periodic Hartree−Fock calculations have been performed on the bcc lattices of Li, Na, K, V, and on the fcc ones of Al, Ca, Sc, Cu in order to investigate the topological properties of the electron charge density and of the electron localization function, ELF. All systems are calculated to be conductors. It is found that the existence of nonnuclear attractors of the electron charge density gradient field first evidenced in lithium clusters is not a prerequisite for metallic behavior. They are missing the V and Cu cells. The topology of ELF is characterized by di- or polysynaptic valence basins. The value of ELF at the valence basin attractors $\eta(\mathbf{r}_a)$ is rather low: typically less than 0.6, which is consistent with an antiparallel pairing close to that of a homogeneous electron gas. At the index 1 saddle points located on the separatrices between valence basins, the ELF value $\eta(\mathbf{r}_s)$ is very close to that at the valence attractors $\eta(\mathbf{r}_a)$. The isosurface $\eta(\mathbf{r}) = \eta(\mathbf{r}_s) - \epsilon$ defines a reducible valence domain which is spread all over the crystal and which forms a tridimensional network of channels. Except for Al, the valence basins have a synaptic order larger than 2. The different topologies of the ELF gradient fields calculated for different metals can be explained by the relative sizes of their core basins. The metallic bond appears to be a partial covalent bond which is often multicentric and is characterized by a low population of the valence basins (less than 1.0 e^-) and by synaptic orders as large as 6.

1. Introduction

The standard description of the metallic bond relies on the band structure theory and implies the closure of the energetical gap between the valence and conduction bands.[1,2] This combined energetical-orbital picture is related to the reciprocal space representation of the crystal. In the absence of a direct space representation, the metallic bond is rather difficult to include in any general chemical theory of the bonding. For example, G. N. Lewis has not considered the metallic bond in his classical textbook,[3] while Pauling describes it as a partial covalent bond between nearest neighbor atomic centers.[4] This covalent description which has been more recently advocated by Anderson et al.[5] and by L. C. Allen and J. Capitani[6] in order to remove the metallic bond from the vocabulary of Chemistry raises, however, the question of the bond (de)localization as well as that of its directionality.

Using the theories expressed in *Atoms in Molecules* of Bader,[7] Gatti et al.[8] demonstrated the presence of nonnuclear attractors (NNAs) of the electron charge density gradient in lithium metal clusters. They also showed how this theory can be easily extended to molecular quantum subspaces which do not enclose a nucleus, and they wonder whether the occurrence of such subspaces might even be a signature of metallic behavior. In a subsequent study Cao et al.[9] found NNAs also in sodium metal clusters and speculated that these attractors should form a connected network in metallic Li and Na which might play some role in the binding and conducting properties of alkali metals. Yet Cao et al. concluded that, possibly, the physical feature necessary for conduction is only a region over which the charge density is relatively flat, with the positive curvature of the bond critical point being very small, thereby ensuring a low kinetic energy per electron. And, as a consequence, the presence of a NNA in the charge density that results when this small positive curvature along the bond path changes sign, might not be essential. Indeed some years later Edgecombe et al.[10] showed that the unusual topological features (i.e., the NNAs) of sodium clusters are removed under the improvement of the basis set and of the correlation scheme whereas they are always present in lithium clusters. The same group carried out an analysis of the charge density gradient field of crystalline lithium and sodium calculated at the periodic Hartree−Fock level.[11] For both metals NNAs are revealed by the topological analysis and they form a connected network in the only case of lithium. The occurrence of NNAs in hcp Be is also a highly debated problem. Experimentally, their absence or their occurrence strongly depends on the model one use to interpret Bragg's diffraction data. If a maximum entropy method (MEM) with a procrystal density as a nonuniform prior is adopted, NNAs are not found,[12] while they are recovered when a MEM analysis with uniform prior or a more conventional multipole model refinement approach is used.[13] More recently, the same set of experimental data has been used by Jayatilaka[15] to invert the Kohn−Sham equations in order to reconstruct Kohn−Sham crystalline orbitals which in the present case do not yield NNAs. On the theoretical side, it has been demonstrated,[14] using either Hartree−Fock or density functional approaches, that the occurrence of NNAs in Be is strongly dependent on basis set choice and closely related to the computed metal cohesive energy. A similar behavior was

10.1021/jp992784c CCC: $19.00
Published on Web 01/19/2000

also observed for Li metal.[16] In the case of Be, the higher is the computed cohesive energy of the metal, the more pronounced is the electron density maximum associated to the NNA. A recent analysis carried out by Martín Pendás et al.[17] has shown that NNAs are not exceptional objects, but result of the properties of the promolecular densities. They are "a normal step in the chemical bonding of homonuclear groups, if analyzed in the appropriate range of internuclear distances". Overall, and up to now, there are neither theoretical arguments nor enough numerical data supporting that the presence of NNAs (connected or not) in periodic solids is the direct space signature of the metallic bond and conductivity.

Another topological approach[18−20] is based on the analysis of the gradient field of the electron localization function ELF of Becke and Edgecombe.[21] As shown by Savin et al.[22] and emphasized by Burdett,[23] the ELF maps of metallic systems present large areas within which the electron localization is nearly constant and close to its jellium value 0.5. These regions are connected one to the other by channels which form infinite one-, two-, and three-dimensional networks according to the conductivity directionality. In the seminal work on the topological analysis of ELF,[18] the metallic bond was characterized by the presence of "unsaturated bonding attractors" and by "reducible localization domains" extending all over the crystal and bounded by an isosurface defined by a value of the localization function close to that of the bonding attractors. Similar extended valence localization domains are also found in intermetallic phases (see the review article on ELF by Savin et al.[24] and references herein particularly[25,26]).

In this paper we present topological analysis of the gradient field of the charge density and of the ELF function carried out on eight metallic cubic structures: on one hand, the bcc phases of Li, Na, K, and V, on the other hand, the fcc phases of Al, Ca, Sc, and Cu. The aim of our work is to show how the topological analysis of ELF constitutes a valid tool for the study of metallic bond in direct space and how this scalar field may provide a signature of metallic behavior which is less elusive and more physically sound than is the presence of nonnuclear maxima or of whatsoever small density curvatures occur along the metal−metal bond paths.

2. Theory.

2.1. Qualitative Topological Theories of Bonding. In the topological theories of the chemical bond[7,18,27] the chemical concepts are defined in terms of the mathematical properties of the gradient vector field of given local functions $f(\mathbf{r})$, called potential functions. The choice of the potential function determines which of the chemical properties may be revealed by the analysis.

The gradient field $\nabla f(\mathbf{r})$ forms a dynamical system (for a comprehensive introduction to the theory of dynamical systems see the textbook of Abraham and Shaw[28]). The analysis of this vector field is based on the analogy with a velocity field:

$$\frac{\partial \mathbf{r}}{\partial t} = \nabla f(\mathbf{r}) \tag{1}$$

The integration of eq 1 enables to build trajectories. Of particular importance for the analysis are the critical points $\mathbf{r}_c$ at which $\nabla f(\mathbf{r})_{\mathbf{r}=\mathbf{r}_c} = 0$. The critical points are characterized by their index which is the number of positive eigenvalues of the Hessian matrix of $f(\mathbf{r})$ in the actual case of gradient dynamical systems. Alternatively, such as in Bader's papers, they are denoted by a couple on integers: the rank (number of non zero eigenvalues of the Hessian matrix) and the signature (the sum of the signs of the eigenvalues). If none of the eigenvalues is zero, the critical point is hyperbolic. There are four kinds of critical points in R^3: (i) attractors of index 0, also denoted (3, −3) critical points, which are the local maxima of the potential function, (ii) saddle points of index 1 or (3, −1), (iii) saddle points of index 2 or (3, 1), (iv) repellors of index 3 or (3, 3) which are the local minima.

The number of critical points satisfies the Poincaré−Hopf formula:

$$\sum_P (-1)^{I(P)} = \chi(M) \tag{2}$$

in which the sum is performed over the critical points, $I(P)$ is the index of the critical point labeled by P, and $\chi(M)$ is the Euler characteristic of the manifold on which the gradient field is bound, i.e., 1 for a molecule, 0 for a periodic system.

The set of points defining the trajectories ending in the neighborhood of a given critical point is the stable manifold of this critical point; that corresponding to out-coming trajectories is its unstable manifold. The dimensions of the stable and unstable manifolds of a critical point of index $I(P)$ are $3-I(P)$ and $I(P)$, respectively. The stable manifold of an attractor is therefore of dimension 3: it is called the basin of the attractor. The stable manifolds of the saddle points of index 1 and 2 are the separatrices of the dynamical system.

The analysis of the gradient dynamical system of a molecular or crystalline local property enables therefore the partition of the space into well-defined adjacent regions, the basins, bounded by the separatrices. The nature of the potential function and the localization of the attractors bring a chemical signification to the basins.

In the case of the *Theory of Atoms in Molecules* the potential function is the electron charge density distribution $\rho(\mathbf{r})$. Except for topical examples, such as the lithium clusters and the lithium crystal, the attractors are located at the nuclei. Therefore a nucleus and the associated basin form an atom in the molecule or in the crystal. In Bader's theory, the unstable manifolds of the critical points of index 1 play an important role as these lines link nuclei two by two. They determine between which atom pairs the chemical bonds are and they are called accordingly bond paths.

The electron localization function ELF[21] is a local measure of the Pauli repulsion.[29] It is expressed in terms of the definite positive kinetic energy density $T_s(\mathbf{r})$, of the von Weizsäcker T_{vW},[30] and of the Thomas−Fermi $T_{TT}(\mathbf{r})$ kinetic energy functionals of the actual system:

$$\eta(\mathbf{r}) = \left(1 + \left[\frac{T_s(\mathbf{r}) - T_{vW}(\mathbf{r})}{T_{TF}(\mathbf{r})}\right]^2\right)^{-1} \tag{3}$$

This function is close to 1.0 in the regions of space where the Fermi hole is large (usually dominated by an antiparallel spin electron pair), it is small where the Fermi hole is narrow, and the value 0.5 corresponds to a situation analogous to that of the homogeneous electron gas. The organization of the basins of ELF provides a picture of the bonding which is consistent with the familiar Lewis theory. There are basically two kinds of basins: on one hand are the core basins encompassing the nuclei with $Z > 2$, and on the other hand, the valence basins the union of which constitute the valence shell of the molecule or of the crystal. The valence basins are characterized by their synaptic order which is the number of core basins with which common boundary is shared.[19] When a proton is located within

a valence basin it is counted as formal core. Monosynaptic basins are associated to lone pairs, disynaptic ones to two center bonds whereas polysynaptic basins are the signature of multicentric bonds. Another important concept is that of domain initially introduced by Mezey.[31] A *f*-localization domain is a volume bounded by the isosurface $\eta(\mathbf{r}) = f$. It is said to be irreducible if it contains one and only one attractor, reducible otherwise.

2.2. Implications of the Jellium Model. The simplest model of a metal is constituted by a periodic array of positively charged ions embedded in a uniform homogeneous electron gas. For this model the attractors of the density gradient field are located on the nuclei of the ion whereas the jellium background gives rise to an infinite number of nonhyperbolic critical points. It is worth noting that such a system is structurally unstable and a more realistic model should be structurally stable and therefore all the critical points should be hyperbolic. However, the jellium model tells us that the values of the potential function at the off-core critical points are confined in a very narrow range independently from their indexes. This expectation is supported by the numerical results of Mei et al. on the lithium and sodium crystals.[11] The fulfillment of the Poincaré-Hopf relationship does not require the existence of NNAs.

In the case of the analysis of the electron localization function, the jellium also gives rise to a continuum of nonhyperbolic critical points which is discretized by the improvement of the model. However, the behavior of ELF is quite different from that of the electron charge density because at the core boundaries the function value is noticeably lower than its jellium values 0.5 whereas at the core attractors it is close to 1. There are necessarily valence basin attractors and the value of ELF defining the reducible localization domain is expected to be very little less than the valence attractor value $\eta(\mathbf{r}_a)$. This reducible localization domain forms a tridimensional network of channels within which the electron localization function and the electron charge density are almost constant and which is consistent with the picture of highly delocalized partial covalent bonds. In this case, partly covalent means that the number of electron per bond is less than 2 because the number of available valence electrons in the unit cell is usually much more less than twice the number of valence basins.

3. Results and Discussion

3.1. Method of Calculation. The calculations of the wave functions have been performed with the periodic Hartree−Fock program CRYSTAL95.[32] The basis functions are derived from the standard 6-31G sets of Pople and co−workers[33,34] and have been designed following the recommendation of the authors of the CRYSTAL programs.[35] In all cases the original sp external shell which is too diffuse has been removed. The 3sp shell is then split into a 21G pattern. The choice of these basis sets has been done in order to have a homogeneous quality thru the series of the investigated metals. At the present state of the art, of all-electron periodic Hartree−Fock calculations performed with localized basis functions, the adopted basis sets should be considered as very good though it is not the case for molecular or cluster calculations. The cutoffs which control the Coulombic and exchange series have been set to 6, 6, 6, and 12 (i.e., the default values), whereas the integration over the Brillouin zone involves 29 *k*-points for both bcc and fcc structures. The lattice parameters are taken from Wyckoff[36] and are given in Table 1. The *Atoms in Molecules* and ELF topological analysis have been made with the TOPOND program developed by one of us (C.G.).[37] In all the calculated systems there is no gap between the valence and conduction bands.

TABLE 1: Structure and Lattice Parameter of the Investigated Metals, Number, and Position of Their Charge Density NNAs

element	structure	a (Å)[36]	n		attractor position
Li	bcc	3.5093	1	(12d)	0, 1/4, 1/2
Na	bcc	4.2906	1	(24h)	u, u, 1/2 $u = 0.152$
K	bcc	5.225	1	(12d)	0, 1/4, 1/2
V	bcc	3.0240	0		
Al	fcc	4.0862	2	(24d)	0, 1/4, 1/4
				(96k)	x, x, z $x = 0.32$, $z = 0.175$
Ca	fcc	5.576	1	(8c)	1/4, 1/4, 1/4
Sc	fcc	4.541	1	(8c)	1/4, 1/4, 1/4
Cu	fcc	3.61496	0		

3.2. Topology of the Electron Charge Density. The number of NNAs and their location is given in Table 1. There is no NNAs for the bcc structure of vanadium and for the fcc lattice of Cu. In principle, the NNAs, when they exist, should be located in the middle of the nearest-neighbor M−M internuclear distances, i.e., the (8c) and (24d) special positions for the $Im\bar{3}m$ and $Fm\bar{3}m$ groups, respectively. This expectation has been verified by Mei et al.[11] for the lithium and sodium crystals; however, our calculations yield different results for these two metals since the non nuclear attractors are found in (12d) and (24h), respectively, for Li and Na. There could be two main causes for this discrepancy. One and probably the most important is the different techniques used to locate the critical points of the electron charge density. The determination of critical points is carried out analytically by TOPOND96, whereas Mei et al. used a graphical technique which implies the interpolation of the function values between grid points. Indeed, the charge density values range in a very narrow interval (7×10^{-4} e^- bohr^{-3} for Li, 2×10^{-5} e^- bohr^{-3} for Na) which hampers the calculations of the derivatives and therefore round off errors might play an important role in the numerical graphical search. The other cause of discrepancy could be the sensitivity of NNA occurrence and location to basis set choice and optimization.[14,16] Among the eight metals only aluminum verifies the expectation; however, it has a second set of NNAs located at the (96k) positions.

Though the critical points of the electron charge density gradient field are hyperbolic, all except the nuclear attractors have Hessian matrix eigenvalues close to zero. Typically, the largest absolute values of such eigenvalues are of the order of 10^{-2} e^- bohr^{-5}. The fulfillment of the hyperbolicity requirement ensures the structural stability of the gradient dynamic system. However, it is conceivable that a rather small variation of the control space parameters (i.e., the nuclear coordinates, the quality of the basis set, ...) should be strong enough to make some of them non hyperbolic and therefore to yield a change of topology thru a bifurcation catastrophe.

3.3. Topology of the Electron Localization Function. Though the closure of the gap between the valence and conduction band is considered as the signature of the conducting state, it has been shown that the insulating state does not require an energy gap.[38] According to Walter Kohn "the insulating characteristics are a strict consequence of electronic localization". In the spirit of Kohn's paper, delocalization means that the wave function "breaks up into a sum of functions which are localized in disconnected regions of the many-particle configuration space". The electron localization function is another tool enabling to decide if the electrons are localized. In fact, when the electrons are localized the free acceleration vanishes and therefore one can expect localized electrons to be "slow" which corresponds to ELF values close to 1. Figure 1

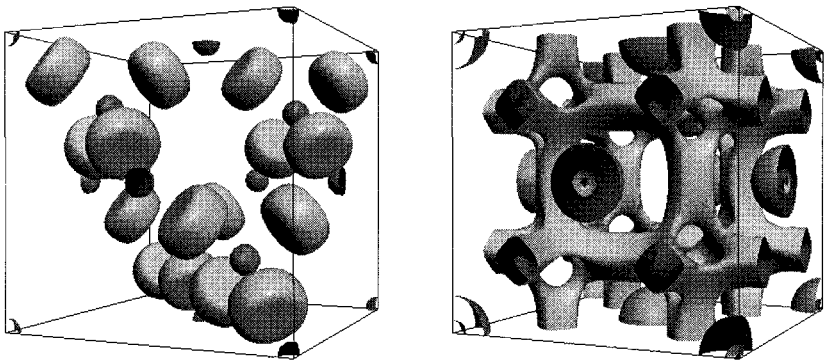

Figure 1. Localization domains of diamond (left) and aluminum. The bounding isosurface are $\eta(\mathbf{r}) = 0.85$ and 0.57 for diamond and aluminum, respectively.

TABLE 2: Localization Function Attractors and Index 1 Critical Points: Positions, Value of ELF at the Attractor $\eta(\mathbf{r}_a)$ and at the Saddle Point $\eta(\mathbf{r}_s)$, Relative Core Volume V_c/V_T, Average Valence Density $\bar{\rho}_v$ (10^{-3} e^- bohr^{-3})

	attractor			saddle point				
element	position		$\eta(\mathbf{r}_a)$	position		$\eta(\mathbf{r}_s)$	V_c/V_T	$\bar{\rho}_v$
Li	(6b)	0, 1/2, 1/2	0.637	(24g)	*x*, 0, 1/2	0.635	0.113	7.7
Na	(24g)	*x*, 0, 1/2	0.563	(24h)	*y*, *y*, 0	0.56	0.165	4.5
K	(24g)	*x*, 0, 1/2	0.536	(24h)	*y*, *y*, 0	0.520	0.278	2.8
V	(24g)	*x*, 0, 1/2	0.60	(24h)	*y*, *y*, 0	0.575	0.485	41.6
Al	(24d)	0, 1/4, 1/4	0.617	(48g)	1/8, 1/4, 1/4	0.583	0.102	29.8
Ca	(8c)	1/4, 1/4, 1/4	0.71	(96j)	0, *y*, *z*	0.525	0.237	9.0
Sc	(8c)	1/4, 1/4, 1/4	0.72	(4b)	1/2, 1.2, 1/2	0.637	0.362	19.8
	(4b)	1/2, 1/2, 1/2	0.67					
Cu	(4b)	1/2, 1/2, 1/2	0.38	(192l)	*x*, *y*, *z*	0.158	0.480	24.1
	(8c)	1/4, 1/4, 1/4	0.2					

displays the localization domains of a typical covalent insulator, the diamond, and of a metallic conductor (aluminum). In diamond the valence attractors at the center of the pastilles between carbon cores coincide with the bond critical points of the charge density. The ELF value at these attractors is close to 1. ($\eta(\mathbf{r})_a$) = 0.97); therefore, the definite positive kinetic energy density is very small and is only due to the Pauli repulsion since the von Weizsäcker functional vanishes at these points. In order to merge the irreducible valence domains into a single reducible one it is necessary to lower the ELF value of the bounding isosurface to $\eta(\mathbf{r})_s = 0.66$. The interval [$\eta(\mathbf{r}_a)$, $\eta(\mathbf{r}_s)$] defines a localization window. In Al, the bounds of the localization window are 0.62 and 0.58. At the attractors the definite positive kinetic energy is larger than for the insulating system. A metallic system is characterized by a rather low value of the valence attractor and by a narrow localization window. As a consequence of the flatness of the ELF function in the interstitial valence region, its critical points have small eigenvalues and therefore a rather weak perturbation may change the nature and the location of the critical points located in this region.

The locations of the valence attractors of the ELF gradient field are reported in Table 2 which shows that there is not a general simple rule relating these positions to the crystallographic space group. In the case of the bcc lattices ($Im\bar{3}m$) there are two different behaviors. Figure 2a−b displays the localization domains of Li and Na. Two isosurfaces have been plotted corresponding to bounding isosurface values close to the valence attractor and to the valence saddle point values, respectively. The valence attractors of lithium are located at the center of the faces in position (6b). The valence basins are truncated octahedra which share boundaries with six core basins, thus their synaptic number is also six. Assuming a core population of 2 e^-, the valence basin population is estimated to be 2/3 e^- from symmetry considerations. The saddle points of index 1 are in position (8c) at the center of the octahedron faces. The value of ELF at these latter points is very close to the attractor value which is the signature of a very large delocalization between valence basins. The isosurface corresponding to a very little inferior value marks the boundary of an infinite tridimensional network of channels within which the localization function is almost constant. The topology of the ELF gradient fields of Na (Figure 2b) K and V derives from that of Li. Each valence attractor of Li has been split into four new attractors which are shifted toward the centers of the edges in position (24g). The basins are truncated tetrahedra corresponding to quarters of the lithium original octahedra. The synaptic order of these basins is 4 and their population 1/6 e^-.

The valence attractors of Al are located between the nearest neighbor nuclei, i.e., in position (24d) and the saddle connections between basins in (48g) yielding channels parallel to the edges of the cube as shown on Figure 1. The valence basins are disynaptic with populations of the order of 1.0 e^-. In the calcium crystal (Figure 1d), the attractors are in the center of the tetrahedra defined by four nearest-neighbor atoms, i.e., in position (8c). The valence basins of synaptic order 4 are truncated hexahedra and their populations are 1 e^-. The connections between basins are ensured by saddle points of index one located in (96j). The topology of scandium shown in Figure 2e is similar, except that there is a second set of attractors in the center of the cube in (4b). The value of the localization function at these latter points is lower than that calculated at position (8c). Finally, in copper Figure 2f the hierarchy of the valence attractors in (8c) and (4b) is reversed, the largest basins corresponding to the (4b) attractors. The synaptic orders of the largest basins of scandium and copper are respectively 4 and 6. It is interesting to note that the populations of the main valence basins in the fcc series are close to 1, which supports the interstitial-electron model proposed by Mo Li and Goddard.[39]

The sizes of the core basins with respect to the lattice volumes explain in part the different topologies calculated for these metals. It must be recalled that the ELF analysis provides a shell structure of the atoms, in particular the 3d subshell of the

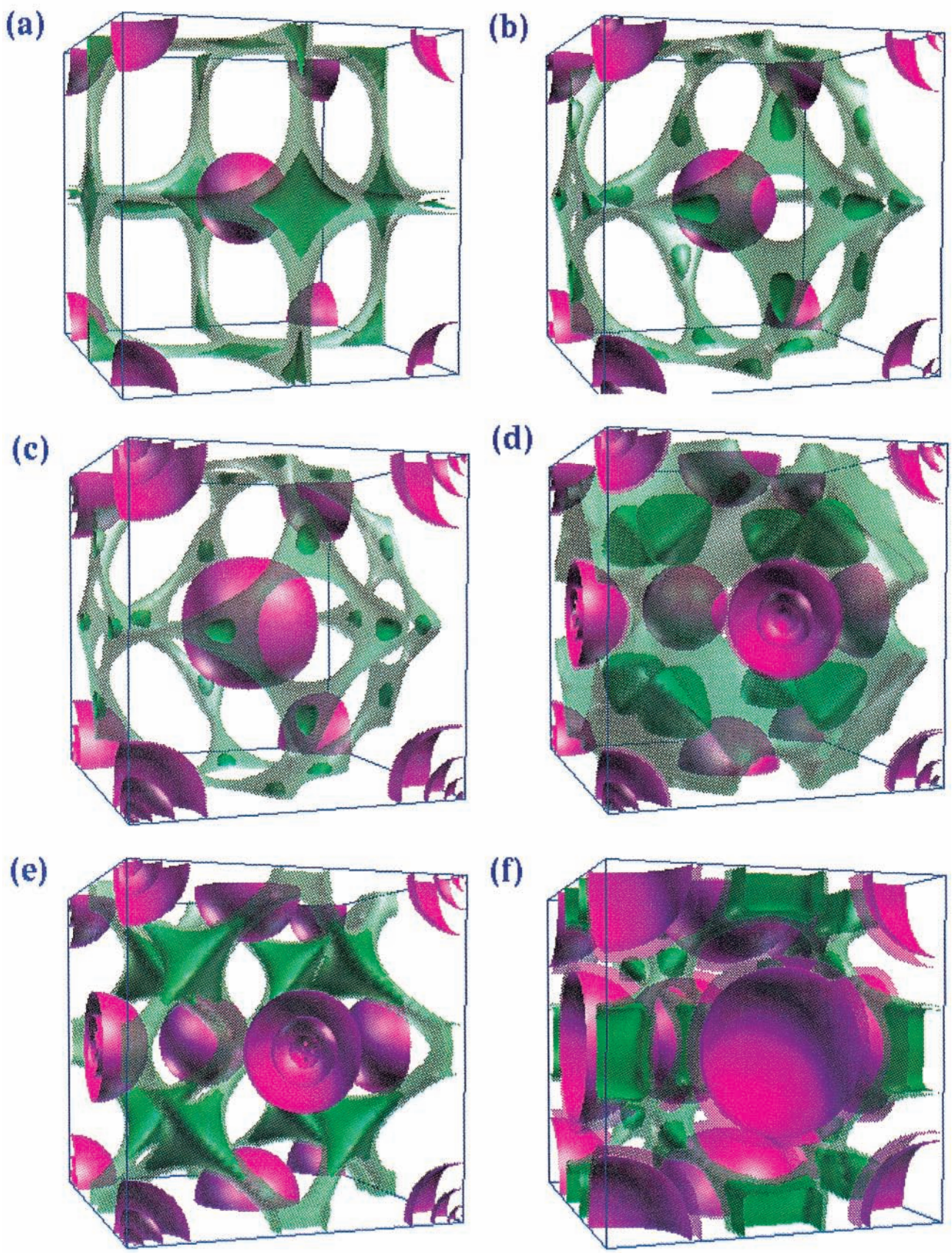

Figure 2. Localization domains of Li (a), Na (b), V (c), Ca(d), Sc (e), and Cu (f). The two bounding isosurfaces have been chosen in order to show the valence attractors and the channels. This figure has been made with the SciAn software.[41] Color code: magenta = core. Green: valence polysynaptic.

transition metals mostly belongs to the core basins. The atomic valence shell populations calculated by Kohout and Savin[40] for Sc, V, and Cu are 2.1, 2.2, and 1.1, respectively. The core radii calculated for the crystalline structures are always in agreement with the values reported by Kohout and Savin.[40] The last entries of Table 2 provides the ratio of the core volume by the cell

volume and the average density of the valence electrons. These latter values are in very good agreement with the local values of the electron charge density calculated at the critical points of this function, with the obvious exception of the (3, −3) critical points associated to nuclei. This behavior confirms the flatness of the charge density over the valence region and indicates that the valence localization domains we defined through ELF just enclose the region where the critical points of $\rho(\mathbf{r})$ are located. In the case of the transition metals, the number of valence electrons on each atom is two for V and Sc, one for Cu. The core shells of the main group elements and of copper are totally filled and therefore exert a kind of "Pauli repulsion pressure" on the valence basin which is stronger than that of Sc and V. The high V_c/V_T ratio of Cu is due to the large volume of an external d-filled core. The location of the valence attractors results of the competition between the core net charge which favors short nucleus−valence attractor distances and the Pauli repulsion which acts in the opposite direction. In the bcc series, the core net charge of alkali is only 1; therefore, the repulsive effects are expected to be the driving force. Accordingly the highest symmetrical position is (6b) as in Li. In this case the valence attractor is surrounded by six nuclei-two at a distance $a/2$, four at $a\sqrt{2}/2$. The valence localization basins are square basis rhombohedra with concave faces. The concavity is more marked for the two faces in front of the nearest cores. As the core size increases, the Pauli repulsion pressure on these faces becomes large enough to make a hole in the domain which splits the central attractor into four attractors each at distances larger than $a/2$ from the nuclei. For V the increased net core charge is compensated for by the largest V_c/V_T ratio in the bcc series. As a consequence, V exhibits the same valence attractors as Na and K. In the fcc series, Al has a net core charge of 3 and a small core. This allows the valence attractor to be at the midpoint of the nearest neighbor distance (i.e., a $a\sqrt{2}/4$ from the nearest nucleus). Ca has net core charges of 2 and a larger core and its valence attractors are in (8c) with a nucleus-attractor distance a $a\sqrt{3}/4$. For Sc, in order to lower the Pauli repulsion exerted on each valence attractor, a secondary set appears in (4b) at $a\sqrt{3}/2$ of the nuclei. For Cu which has the largest core and the least core net charge, this latter set of attractors becomes the main one.

4. Conclusion

The analysis of the gradient fields of the electron charge density of metals is consistent with the expectations which can be made from the homogeneous electron gas model. On one hand, the properties of the electron density are almost constant in the valence regions as indicated by the weak magnitude of the eigenvalues of the Hessian matrices calculated at the critical points. On the other hand, the location of the attractors is often different from those found in covalent molecules and crystals. The analysis of the electron charge density confirms[10,11] that NNAs are not a necessary feature of metallic behavior. In our results we find conducting materials with and without such attractors. It may be argued that they might become visible upon improvement of the computational scheme. However, the important point is that it is possible to calculate a model conductor without NNAs.

The analysis of the electron localization function provides a picture of the metallic bond which is a generalization of that of Pauling.[4] The metallic bond is basically a partial covalent bond. Here partial does not refer to any possible ionic contribution but rather to the fact that the basin populations are always very low (typically less than 1 e^-). This is due to the high coordination of the atoms in the crystal and to the strong Pauli repulsion arising from the cores which tends to increase the number or the synaptic order of the valence attractors. Moreover, the reducible valence localization domains (i.e., which encompass at least two valence attractors) form an infinite network over the whole crystal. The channels built in this way can be considered as the region of the space within which the conduction takes place. An argument in favor of this interpretation is provided by calculations of anisotropic conductors, such as gallium, for which the channels form parallel 2-dimensional networks. Though, calculations of the variance of the basin population have not be performed (up to now this is only possible for molecules) the values of ELF at its valence attractors and at its saddle points are a strong indication of the electron delocalization.

Though the gradient dynamical systems of the charge density and of ELF are structurally stable because their critical points are hyperbolic, a rather weak variation of the control space parameters should induce a significant topological change. This can be achieved by small displacements of the nuclei. Work is in progress in order to provide a direct space visual representation of the electron−phonon interaction by the technique presented here.

References and Notes

(1) Kittel, C. *Quantum Theory of Solids*; John Wiley and Sons: New York, 1963.
(2) Ashcroft, N. W.; Mermin, N. D. *Solid State Physics*; Saunders College Publishing: Fort Worth, 1976.
(3) Lewis, G. N. *Valence and the Structure of Atoms and Molecules*; Dover: New York, 1966.
(4) Pauling, L. *The Nature of the Chemical Bond*; Cornell University Press: Ithaca, 1948.
(5) Anderson, W. P.; Burdett, J. K.; Czech, P. T. *J. Am. Chem. Soc.* **1994**, *116*, 8808.
(6) Allen, L. C.; Capitani, J. F. *J. Am. Chem. Soc.* **1994**, *116*, 8810.
(7) Bader, R. F. W. *Atoms in Molecules: A Quantum Theory*; Oxford University Press: Oxford, 1990.
(8) Gatti, C.; Fantucci, P.; Pacchioni, G.; *Theor. Chim. Acta (Berlin)* **1987**, *72*, 433.
(9) Cao, W. L.; Gatti, C.; MacDougall, P. J.; Bader, R. F. W. *Chem. Phys. Lett.* **1987**, *141*, 380.
(10) Edgecombe, K.; Esquivel, R.; Smith, V. H.; Muller-Plathe, F. J.; *J. Chem. Phys.* **1992**, *97*, 2595.
(11) Mei, C.; Edgecombe, K. E.; Smith, V. H., Jr.; Heilingbrunner, A. *Int. J. Quantum Chem.* **1993**, *48*, 287.
(12) de Vries, R. Y.; Briels, W. J.; Feil, D. *Phys. Rev. Lett.* **1996**, *77*, 1719.
(13) Iversen, B. B.; Larsen, F. K.; Souhassou, M.; Takata, M. *Acta Crystallogr. Sect. B* **1995**, *51*, 580.
(14) (a) Gatti, C.; Cargnoni, F. *Extended Abstracts, III Convegno Nazioanle di Informatica Chimica*, Napoli, Italy. February 27−March 1, 1997; pp 125−128. (b) Gatti, C.; et al. In preparation.
(15) Jayatilaka, D.; *Phys. Rev. Lett.* **1998**, *80*, 798.
(16) By using the 8s1p/(611/1) basis set from Dovesi, R.; Ferrero, R.; Pisani, C.; Roetti, C. *Z. Phys. B* **1983**, *51*, 195−203, one may find, according to the value adopted for the outermost p function, no nonnuclear attractor (NNA), one NNA in (8c), or two NNA along the internuclear axis joining two first neighbors with an intervening saddle point in (8c).
(17) Martín Pendás, A.; Blanco, M. A.; Mori Sánchez, A. C. P.; na, V. L. *Phys. Rev. Lett.* **1999**, *83*, 1930.
(18) Silvi, B.; Savin, A. *Nature* **1994**, *371*, 683.
(19) Savin, A.; Silvi, B.; Colonna, F. *Can. J. Chem.* **1996**, *74*, 1088.
(20) Noury, S.; Colonna, F.; Savin, A.; Silvi, B. *J. Mol. Struct.* **1998**, *450*, 59.
(21) Becke, A. D.; Edgecombe, K. E. *J. Chem. Phys.* **1990**, *92*, 5397.
(22) Savin, A.; Jepsen, O.; Flad, J.; Andersen, O. K.; Preuss, H.; von Schnering, H. G. *Angew. Chem., Int. Ed. Engl.* **1992**, *31*, 187.
(23) Burdett, J. K. *J. Phys. Chem.* **1996**, *100*, 13263.
(24) Savin, A.; Nesper, R.; Wengert, S.; Fässler, T. F.; *Angew. Chem., Int. Ed. Engl.* **1997**; *36*, 1809.
(25) Häussermann, U.; Wengert, S.; Nesper, R.; *Angew. Chem., Int. Ed. Engl.* **1994**, *33*, 2069.
(26) Grin, Y.; Wedig, U.; Wagner, F.; von Schnering, H. G.; Savin, A. *J. Alloys Compd.* **1997**, *255*, 203.

(27) Gadre, S. R.; Sears, S. B.; Chakravorty, S. J.; Bendale, R. D. *Phys. Rev.* **1985**, *A32*, 2602.

(28) Abraham, R. H.; Shaw, C. D. *Dynamics the Geometry of Behavior*; Addison Wesley: 1992.

(29) Savin, A.; Becke, A. D.; Flad, J.; Nesper, R.; Preuss, H.; von Schnering, H. G. *Angew. Chem., Int. Ed. Engl.* **1991**, *30*, 409.

(30) von Weizsäcker, C. F. *Z. Phys.* **1935**, *96*, 431.

(31) Mezey, P. G. *Can. J. Chem.* **1993**, *72*, 928.

(32) Dovesi, R.; Saunders: V. R.; Roetti, C.; Causà, M.; Harrison, N. M.; Orlando, R. CRYSTAL95, User's manual; 1996.

(33) Hehre, W. J.; Stewart, R. F.; Pople, J. A. *J. Chem. Phys.* **1969**, *51*, 2657.

(34) Rassolov, V. A.; Pople, J. A.; Ratner, M. A.; Windus, T. L. *J. Chem. Phys.* **1998**, *109*, 1223.

(35) Pisani, C.; Dovesi, R.; Roetti, C. *Hartree−Fock Ab Initio Treatment of Crystalline Systems*; Lecture Notes in Chemistry 48; Springer-Verlag: Berlin, 1988.

(36) Wyckoff, R. W. G. *Crystal Structures*; Robert E. Krieger, Malabar 1986.

(37) Gatti, C. Topond 96 user's manual, 1997.

(38) Kohn, W. *Phys. Rev.* **1964**, *133*, A171.

(39) Mo Li; Goddard, W. A., III; *Phys. Rev.* **1989**, *B40*, 12155.

(40) Kohout, M.; Savin, A. *Int. J. Quantum Chem.* **1996**, *60*, 875.

(41) Pepke, E.; Murray, J.; Lyons, J.; Hwu, T.-Z. *Scian*; Supercomputer Computations Research Institute, Florida State University: Tallahassee, FL, 1993.